

Constructing a Loess Landslide Run-Out Prediction Input Parameter Database through Multi-Objective Optimization Back Analysis

Peng Zeng¹, Lin Zhang², Liangfu Zhao³, Xiaoping Sun⁴, Xiujun Dong⁵

¹State Key Laboratory of Geohazard Prevention and Geoenvironment Protection (Chengdu University of Technology), Chengdu, China.

E-mail: zengpeng15@cdut.edu.cn

²State Key Laboratory of Geohazard Prevention and Geoenvironment Protection (Chengdu University of Technology), Chengdu, China.

E-mail: zhanglin97@stu.cdut.edu.cn

³State Key Laboratory of Geohazard Prevention and Geoenvironment Protection (Chengdu University of Technology), Chengdu, China.

E-mail: zhaoliangfu@stu.cdut.edu.cn

⁴State Key Laboratory of Geohazard Prevention and Geoenvironment Protection (Chengdu University of Technology), Chengdu, China.

E-mail: sunxiaoping@stu.cdut.edu.cn

⁵State Key Laboratory of Geohazard Prevention and Geoenvironment Protection (Chengdu University of Technology), Chengdu, China.

E-mail: 16704937@qq.com

Abstract:Loess landslides pose a great physical and environmental threat to communities around the Heifangtai Terrace in Gansu Province, China. Evaluating the potentially affected area provides a basis for loess landslide risk assessment and management. However, rheological input parameters for loess landslide run-out analyses involve large uncertainties that often result in biased predictions. To that end, this study collected 20 loess flowslides occurred from 2015 to 2019 in the Heifangtai Terrace. A friction model embedded in Mass flow was used to simulate the run-out behavior of loess landslides. The accumulation depths of several control points located on the accumulation area were employed as observation information. A multi-objective optimization back analysis method using a non-dominated solution genetic algorithm (NSGA-II) was proposed to calibrate the optimal rheological parameters for each landslide, thus obtaining a parameter database including 20 datasets for statistical analyses. The proposed back analysis method and obtained rheological parameter database can be used for conducting future landslide run-out prediction in the Heifangtai area.

Keywords: Loess flowslide; Multi-objective optimization; Back analysis; Rheological parameter database; Statistical analysis

1 Introduction

Landslides is one of the major geological disasters, causing many casualties and severe property losses (Dai et al. 2002). In the Loess Plateau in northwest China, many loess landslides occur because of loess collapsibility, agricultural irrigation, and soil erosion (Xu et al. 2014). To decrease their societal impact, it is necessary to conduct landslide risk assessments and implement appropriate mitigation strategies (Peng et al. 2015). Predicting and evaluating the possible spatial impact of potential landslides is a key issue in quantitative risk assessment (Zeng et al. 2021) and is also considered an important means of disaster prevention and reduction (Ho and C.F. 2006, Westen et al. 2006, Zhou et al. 2020).

Numerical methods (e.g., Massflow (Ouyang et al. 2013) employed in this study) provide comprehensive information on run-out intensities, and have been widely employed to simulate the run-out process of landslides. However, the rheological parameters (i.e., the effective residual friction angle ϕ' and pore pressure ratio r_u of friction model embedded in Massflow) for run-out analysis involve large uncertainties that result in biased predictions. Therefore, in this study, we focus on the loess flowslides in the Heifangtai Terrace, and collected pre- and post-sliding high-resolution unmanned aerial vehicle (UAV) point cloud data for 20 historical flowslides that occurred during the past decade. A non-dominated sorting genetic algorithm (NSGA-II)-based multi-objective optimization back analysis method is employed to calibrate the rheological parameters of each landslide and construct parameter database for a reliable probabilistic run-out analysis.

2 Geological background of the study area

Heifangtai Terrace (Figure 1) is located at the intersection of Yellow River and Huangshui River, and being about 40 km west of Lanzhou City, Gansu Province, China (Peng et al. 2018, Qi et al. 2018). The Heifangtai Terrace

covers a total area of 13.7 km², and is divided by Hulang gully into Heitai Terrace and Fangtai Terrace (Qi, et al. 2018). It contains four layers from top to bottom: Malan loess with a thickness of 25–48 m; silty clay with a thickness of 3–19 m, which is considered impermeable; a 1–6 m thick gravel layer; and sandstone and mudstone as the terrace base (Sun et al. 2021). In order to meet the production and living needs of immigrants, the local government built a number of pumping projects to pump water from the Yellow River up to Heifangtai Terrace for agricultural irrigation (Gu et al. 2019).

Since 1968, more than 200 loess landslides were observed and recorded in Heifangtai Terrace. The loess flow slide caused by the sharp rise of groundwater level is found to be the most common type of loess landslide in Heifangtai Terrace, and it has the characteristics of liquefaction, fluidization, high speed, and long run-out distance (Peng, et al. 2018, Qi, et al. 2018, Xu, et al. 2014). For instance, on April 29, 2015, a high-speed flow slide occurred in Dangchuan village, Heifangtai, with a volume of about $4.5 \times 10^5 \text{ m}^3$ and a coverage area of $1.1 \times 10^5 \text{ m}^2$ (Qi, et al. 2018). 14 buildings, 3 factories and a more than 80 acres of farmland were destroyed, and the direct economic loss was as high as 56.5 million RMB. On February 19, 2017, a flow slide occurred in Dangchuan village, Heifangtai, with a volume of about $1.3 \times 10^5 \text{ m}^3$ and a coverage area of $5.6 \times 10^4 \text{ m}^2$ (Qi, et al. 2018), resulted in residential farmland, tap water in three villages being destroyed, and the water supply of more than 6000 households were blocked. From 2015 to 2019, we recorded 20 flow slides (Figure 1) and obtained their geological and geotechnical information through field investigation for this study. In the following sections, we illustrate the application of the multi-objective optimization method to calibrate the rheological parameters (i.e., φ' and r_u) for each loess flow slide to obtain the statistical information.

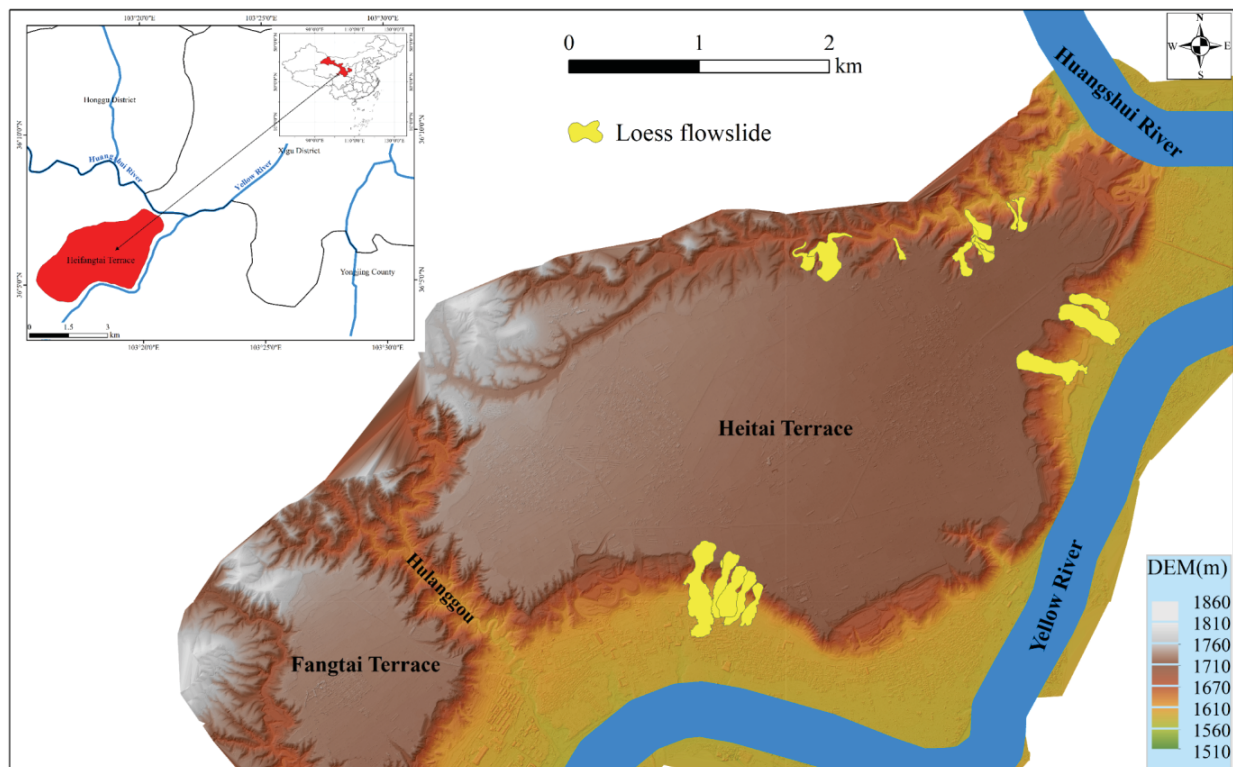


Figure 1. Distribution of loess flowslides that occurred between 2015 and 2019 in the Heifangtai Terrace

3 Multi-objective optimization back analysis for rheological parameters calibration

3.1 Objectivemismatch functions

Let $\theta = [\varphi', r_u]^T$ denote a vector of rheological parameters to be calibrated in a dynamic numerical model and let T represent the matrix transposition. The prior mean values (i.e., $\mu_0 = [\mu_{\varphi'}, \mu_{r_u}]^T = [34.6, 0.5]^T$) and standard deviations (i.e., $\sigma_0 = [\sigma_{\varphi'}, \sigma_{r_u}]^T = [3.45, 0.1]^T$) were obtained by Sun, et al. (2021) and Zeng, et al. (2021). The target of the back analysis is to determine an optimal rheological parameter set that results in actual observed characteristics of the loess flow slide from the obtained prior knowledge. These characteristics usually include the impact area, run-out velocity, run-out distance, and accumulation depth (Aaron et al. 2019). In this study, to control the geometric characteristics of flow slides, we used accumulation depths at different spatial locations in the accumulation area as observation information. Flowslide CJ#8-6 was taken as an example for illustrating the selected observation points, as showed in Figure 2.

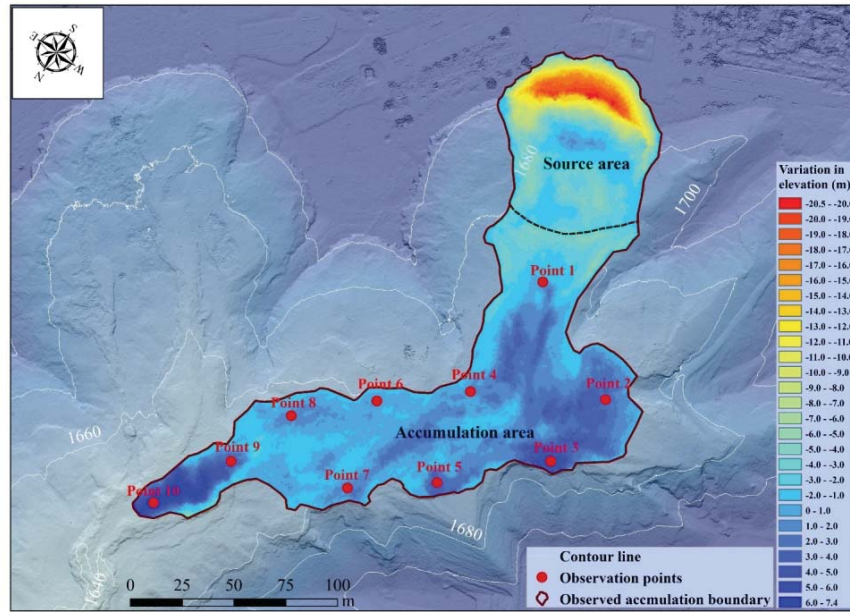


Figure 2. Accumulation depths and distribution of observation points of flowslide CJ#8-6

Let \mathbf{H} denote a set of observed accumulation depths after the flowslide, given as

$$\mathbf{H} = [h_1, L, h_i, L, h_n]^T \quad (1)$$

where h_i is the observation depth at the i th location and n is the number of observation locations. Given a set of rheological parameters, the landslide run-out process was reproduced using MassFlow. Let $\mathbf{Y}(\boldsymbol{\theta})$ denote a set of simulated accumulation depths located in the observation locations, given as

$$\mathbf{Y}(\boldsymbol{\theta}) = [y_1(\boldsymbol{\theta}), L, y_i(\boldsymbol{\theta}), L, y_n(\boldsymbol{\theta})]^T \quad (2)$$

where $y_i(\boldsymbol{\theta})$ denotes the simulated accumulation depth at the i th location. Thus, the first objective function considering the difference between the observation and simulation results can be written as

$$f_1(\boldsymbol{\theta}) = [\mathbf{H} - \mathbf{Y}(\boldsymbol{\theta})]^T [\mathbf{H} - \mathbf{Y}(\boldsymbol{\theta})] \quad (3)$$

Meanwhile, different combinations of φ' and r_u may produce similar or even the same value of $f_1(\boldsymbol{\theta})$, thus resulting in infinite solutions for minimizing $f_1(\boldsymbol{\theta})$. Theoretically, an optimal $\boldsymbol{\theta}$ should be within its prior information range and close to its prior mean value. Therefore, the second objective function can be written as

$$f_2(\boldsymbol{\theta}) = \left[\frac{\boldsymbol{\theta} - \boldsymbol{\mu}_0}{\boldsymbol{\sigma}_0} \right]^T \left[\frac{\boldsymbol{\theta} - \boldsymbol{\mu}_0}{\boldsymbol{\sigma}_0} \right] \quad (4)$$

However, there are some conflicts to minimize $f_1(\boldsymbol{\theta})$ and $f_2(\boldsymbol{\theta})$ simultaneously. This means that while one decreases, the other may increase. It is impossible to obtain an ideal optimal solution that makes $f_1(\boldsymbol{\theta}) = 0$ and $f_2(\boldsymbol{\theta}) = 0$ simultaneously. However, it is feasible to make $f_1(\boldsymbol{\theta})$ and $f_2(\boldsymbol{\theta})$ as small as possible using multi-objective optimization.

3.2 Multi-objective optimization

The multi-objective optimization problem considered in this paper can be described as

Minimize $f_1(\boldsymbol{\theta})$ and $f_2(\boldsymbol{\theta})$

$$\boldsymbol{\theta} = [\varphi', r_u] \text{ subject to: } \begin{cases} \varphi' \in [L_{\varphi'}, U_{\varphi'}] \\ r_u \in [L_{r_u}, U_{r_u}] \end{cases} \quad (5)$$

where $L_{\varphi'}$ and L_{r_u} are the lower bounds of the rheological parameters and $U_{\varphi'}$ and U_{r_u} are the upper bounds of the rheological parameters. In this study, the NSGA-II was used to identify the Pareto optimal solutions (i.e., non-dominated solutions) of the objective mismatch functions $f_1(\boldsymbol{\theta})$ and $f_2(\boldsymbol{\theta})$.

3.2 Multi-objective optimization decision

Once the optimization process was completed, a set of final non-dominated solutions can be obtained. In the decision making of practical problems, it is necessary to select the most suitable solution from the Pareto optimal frontier. In this study, the linear programming technique for multidimensional analysis of preference (LINMAP) was employed to make decisions for selecting the final optimal solution in an objective manner.

Before applying the decision-making method, we need to make each objective function value dimensionless for scale consistency and ease of comparison. This can be realized using the Euclidean method (Maputi and Arora 2020, Sayyaadi and Mehrabipour 2012).

$$\mathbf{T}_j = \frac{\mathbf{P}_j}{\sqrt{\sum_{j=1}^m (\mathbf{P}_j^T \mathbf{P}_j)}} \quad (6)$$

where $\mathbf{P}_j = [f_{1,j}(\boldsymbol{\theta}), f_{2,j}(\boldsymbol{\theta})]^T$ is the Pareto optimal frontier, m is the number of non-dominated Pareto optimal frontier solutions, and \mathbf{T}_j is a dimensionless matrix.

The LINMAP decision-making method computes the distance between each dimensionless solution of the Pareto optimal frontier \mathbf{T}_j and the ideal solution \mathbf{A} :

$$d_{j+} = \|\mathbf{T}_j - \mathbf{A}\| \quad (7)$$

Then, the Pareto optimal frontier with the minimum distance from the ideal solution is selected as the final optimal solution, given as

$$\mathbf{T}_{j,\text{optimal}} \equiv \mathbf{T}_j \in \min(d_{j+}) (1 \leq j \leq m) \quad (8)$$

Finally, the corresponding input parameter $\boldsymbol{\theta}$ that results in $\mathbf{T}_{j,\text{optimal}}$ is considered as the calibrated rheological parameter set and can be used in probabilistic run-out predictions of loess flowslides.

4 Rheological parameters database and statistical analysis

The multi-objective optimization back analysis method discussed in Chapter 3 was applied to 20 flowslides recorded in Heifangtai Terrace for rheological parameters calibration. The obtained Pareto optimal frontiers are shown in Figure 3. The calibrated rheological parameters are listed in Table 1.

Statistical analysis was applied to the calibrated values of the rheological parameters φ' and r_u listed in Table 1. The mean and standard deviation of φ' were 33.54° and 1.10° , respectively, and the mean and standard deviation of r_u were 0.5604 and 0.0699, respectively. Compared with the prior information of the rheological parameters, the mean value of φ' was slightly decreased, while the mean value of r_u was slightly increased, and their standard deviations were both reduced. This implies that landslides obeying the same failure mode (e.g., flowslide caused by loess liquefaction considered in this study) exhibit similar run-out characteristics, and their calibrated rheological parameters are close to each other. It also indicates that a detailed landslide type classification may help to better understand the run-out behavior and contributes to potential landslide prediction with less uncertainty.

Table 1. Calibrated rheological parameters for the 20 loess flowslides

Flowslide	DC#2-3	DC#3-4	DC#3-6	DC#4-3	DC#5-2	DC#9-3	JY#6-11
φ' ($^\circ$)	32.21	33.18	33.51	34.87	35.50	34.13	34.13
r_u	0.6465	0.5218	0.5372	0.5058	0.4538	0.5277	0.5440
Flowslide	JJ#4-3	JJ#7-1	CJ#3-6	CJ#3-7	CJ#5-1	CJ#6-6	CJ#6-7
φ' ($^\circ$)	32.76	33.78	33.39	34.53	34.98	32.85	33.47
r_u	0.6119	0.5470	0.5079	0.4858	0.5109	0.6119	0.5552
Flowslide	CJ#6-8	CJ#7-1	CJ#8-6	CJ#8-7	MS#2-4	MS#10-1	
φ' ($^\circ$)	32.66	33.27	31.07	31.73	34.28	34.41	
r_u	0.5777	0.5590	0.7449	0.7003	0.5458	0.5124	

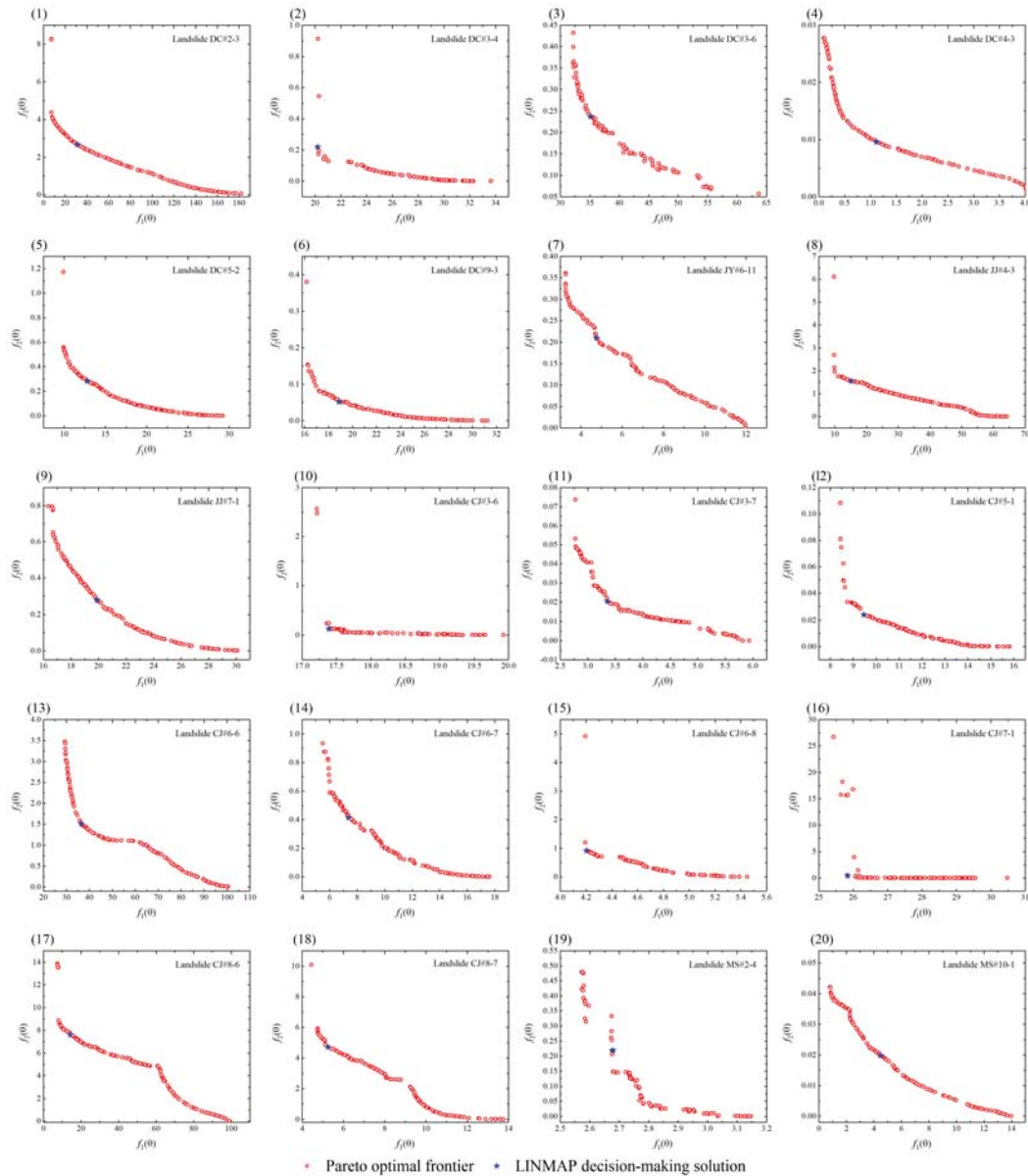


Figure 3. Pareto optimal frontier and decision-making solution of 20 flowslides

The Pearson correlation coefficient(Li et al. 2012)between φ' and r_u was also investigated based on 20 calibrated results and showed that φ' and r_u were negatively correlated, with a correlation coefficient of $\rho = -0.9161$.Finally, the Kolmogorov–Smirnov (K–S) test(Massey 1951)was applied based on the calibrated results to confirm that the generalized extreme value distribution was acceptable for both φ' and r_u . All the statistical information for φ' and r_u is shown in Figure 4.

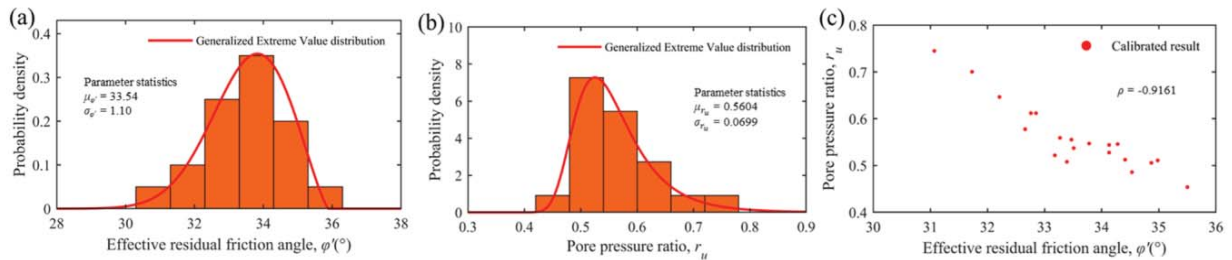


Figure 4.Statistical information of the calibrated φ' and r_u

5 Summary

This study integrated both the prior information of rheological parameters and the accumulation depths of 20 loess flow slides induced by continuous agricultural irrigation in the Heifangtai Terrace and proposed a multi-

objective optimization-based back analysis method to calibrate the rheological parameters (i.e. the effective residual friction angle φ' and the pore pressure ratio r_u). Based on the computed results, the following conclusions are drawn.

(1) The statistical information of rheological parameters showed that the effective residual friction angle φ' had a mean of 33.54° and a standard deviation of 1.10° , and the pore pressure ratio r_u had a mean of 0.5604 and a standard deviation of 0.0699. They were negatively correlated, with a correlation coefficient of -0.9161.

(2) The generalized extreme value distributions were acceptable for both φ' and r_u . This provides a valuable probability distribution for loess flow slides run-out analyses.

(3) The proposed method can be applied to other areas where similar historical landslides are well documented to obtain statistical information on rheological parameters for reliable landslide run-out prediction and risk assessment.

Acknowledgments

This research was supported by the National Natural Science Foundation of China (Project No. 41977224) and the State Key Laboratory of Geohazard Prevention and Geoenvironment Protection (Project No. SKLGP2020Z013 and SKLGP2021K001). Their financial support is greatly appreciated.

References

- Aaron J, McDougall S and Nolde N. (2019). Two methodologies to calibrate landslide runout models. *Landslides*, 16, 907-920.
- Dai FC, Lee CF and Ngai YY. (2002). Landslide risk assessment and management: An overview. *Eng Geol*, 64, 65-87.
- Gu T-f, Zhang M-s, Wang J-d, Wang C-x, Xu Y-j and Wang X. (2019). The effect of irrigation on slope stability in the heifangtai platform, gansu province, china. *Eng Geol*, 248, 346-356.
- Ho JD and C.F. C. (2006). Life risk assessment of landslide disaster using spatial prediction model. *Journal of Environmental Impact Assessment*, 15, 373-383.
- Li D, Tang X, Zhou C and Phoon K-K. (2012). Uncertainty analysis of correlated non-normal geotechnical parameters using gaussian copula. *Science China Technological Sciences*, 55, 3081-3089.
- Maputi ES and Arora R. (2020). Multi-objective optimization of a 2-stage spur gearbox using nsga-ii and decision-making methods. *Journal Of The Brazilian Society Of Mechanical Sciences And Engineering*, 42, 477.
- Massey FJ. (1951). The kolmogorov-smirnov test for goodness of fit. *J Amer Statist Assn*, 46, 68-78.
- Ouyang C, He S, Xu Q, Luo Y and Zhang W. (2013). A maccormack-tvd finite difference method to simulate the mass flow in mountainous terrain with variable computational domain. *Comput Geosci*, 52, 1-10.
- Peng D, Xu Q, Liu F, He Y, Zhang S, Qi X, Zhao K and Zhang X. (2018). Distribution and failure modes of the landslides in heitai terrace, china. *Eng Geol*, 236, 97-110.
- Peng L, Xu S, Hou J and Peng J. (2015). Quantitative risk analysis for landslides: The case of the three gorges area, china. *Landslides*, 12, 943-960.
- Qi X, Xu Q and Liu F. (2018). Analysis of retrogressive loess flowslides in heifangtai, china. *Eng Geol*, 236, 119-128.
- Sayyaadi H and Mehrabipour R. (2012). Efficiency enhancement of a gas turbine cycle using an optimized tubular recuperative heat exchanger. *Energy*, 38, 362-375.
- Sun X, Zeng P, Li T, Wang S, Jimenez R, Feng X and Xu Q. (2021). From probabilistic back analyses to probabilistic run-out predictions of landslides: A case study of heifangtai terrace, gansu province, china. *Eng Geol*, 280, 105950.
- Westen CJ, Asch TWJ and Soeters R. (2006). Landslide hazard and risk zonation—why is it still so difficult? *Bull Eng Geol Environ*, 65, 167-184.
- Xu L, Iqbal J, Dai F, Tu X, Tham L and Zhou Y. (2014). Landslides in a loess platform, north-west china. *Landslides*, 11, 993-1005.
- Zeng P, Sun X, Xu Q, Li T and Zhang T. (2021). 3d probabilistic landslide run-out hazard evaluation for quantitative risk assessment purposes. *Eng Geol*, 293, 106303.
- Zhou Q, Xu Q, Peng D, Fan X, Ouyang C, Zhao K, Li H and Zhu X. (2020). Quantitative spatial distribution model of site-specific loess landslides on the heifangtai terrace, china. *Landslides*, 18, 1163-1176.